Skyrme Hartree-Fock calculations and the structure of exotic nuclei

W. A. Richter
Department of Physics, University of Stellenbosch,
Stellenbosch 7600, South Africa

B. A. Brown
Department of Physics and Astronomy
and National Superconducting Cyclotron Laboratory, Michigan State University,
East Lansing, Michigan 48824-1321, USA

Abstract

The study of the structure of exotic nuclei has necessitated the use of interactions which have good global properties, such as Skyrme forces, in self-consistent Hartree-Fock calculations using a mean-field approach. The newer SKX parameterization has been particularly successful. To take into account nuclear correlations a successful attempt has been made to combine the best features of the nuclear shell and Hartree-Fock models and to apply it to the Ca isotopes. The Skyrme Hartree-Fock method has also been applied successfully to calculate Coulomb displacement energies and describe the well-known Nolen-Schiffer anomaly, as well as nuclear charge density distributions and charge radii for a large variety of nuclei, neutron and proton density distributions for the Na isotopes, and to more accurate estimates of the masses of proton-rich nuclei relevant to the rp-process. Calculated interaction cross-sections and rms matter radii for nuclei with Z = 2-12 on a ^{12}C target, based on a Glauber model, with matter densities obtained from the Skyrme Hartree-Fock model, gave excellent agreement with experiment. An overview of all these applications are given in the present paper.

1 Introduction

During recent years theoretical work on nuclear structure has progressively shifted to the study of nuclei far from stability, or so-called exotic nuclei. The present work is part of a general investigation into the properties of nuclei far from stability. The logical starting point of such an investigation are the standard models of nuclear structure developed for stable nuclei, e.g. the Hartree-Fock model and the nuclear shell model. From these models one can then extrapolate into regions further from the valley of stability, and ultimately to the neutron and proton driplines. From discrepancies encountered in the extrapolations one can learn about the shortcomings of the models, and hopefully apply appropriate corrections. This is a general strategy for attacking the problem of nuclei far from stability. For a description of global properties such as ground-state binding energies, nuclear radii and densities a mean-field approach works well, such as the Hartree-Fock method with Skyrme interactions, and this will be the basis of our calculations in this work. However, we should be mindful of the limitations of the model, since it known, for example, that for local properties such as excitation energies, nuclear moments and transition strengths, the nuclear shell model with its cognizance of nucleon correlations has to be invoked. We have attempted to compensate for this shortcoming in various

ways, for example by combining the best features of the nuclear shell and Hartree-Fock models, or by using nucleon occupation numbers derived from shell-model calculations when calculating charge density distributions.
Recently a new Skyrme interaction has been obtained [1] from fits to a large body of data related to nuclear ground state properties, which include binding energies, rms charge radii and single-particle energies. Some of the most exotic nuclei studied to date have been included in order to improve the reliability for predictions towards the drip lines. The main new ingredient which distinguishes it from many other Skyrme interactions in the literature is the emphasis on the single-particle energies, of which 79 are included in the fits. The second ingredient is a consistent formulation for both proton-rich and neutron-rich nuclei. Also a more generalized form for the spin-orbit interaction has been adopted and constraints have placed on the Skyrme parameters which are related to nuclear and neutron matter properties. This interaction has been mainly used in this work, and in some cases we use older parametrizations that work particularly well in specific situations.
Our calculations have been applied to a variety of situations which are summarized here:
The calculation of neutron radii
Combining the shell model and the Hartree-Fock method
Coulomb displacement energies
Masses of proton-rich nuclei relevant to the astrophysical rp process
Interaction cross-sections for light neutron-rich nuclei
Nuclear charge densities and rms radii
Q-values for alpha decay of superheavy nuclei
Each of these applications will be discussed in the sections that follow.

2 The calculation of neutron radii

In a GSI experiment Argon isotopes were accelerated and directed at a Be production target to produce a variety of Na isotopes [2]. The rms matter radii were extracted using a Glauber-model analysis of interaction cross-section data. The rms neutron radii were deduced using estimates of proton rms radii from isotope shifts. Comparing the rms neutron radii with our calculated values [3] in Fig. 1 shows that good general agreement is obtained. Our calculations are extended beyond the available experimental values to indicate a drip line at N=34, or A=45.

3 Combining the shell model and the Hartree-Fock method

A new method was developed to combine the large-basis shell-model and Hartree-Fock methods [4]. The Hartree-Fock method is used to obtain the absolute uncorrelated binding energies, a starting set of single-particle energies (SPE) and the single-particle radial wave functions. The shell-model Hamiltonian is modified to remove the monopole terms and these are replaced by Hartree-Fock single-particle energies obtained as a function of mass number. The shell-model is then used to calculate the ground-state correlation energy and the excited state spectrum. The HF SPE are not always in perfect agreement with the properties of the closed-shell nuclei, and one should expect that the actual SPE for

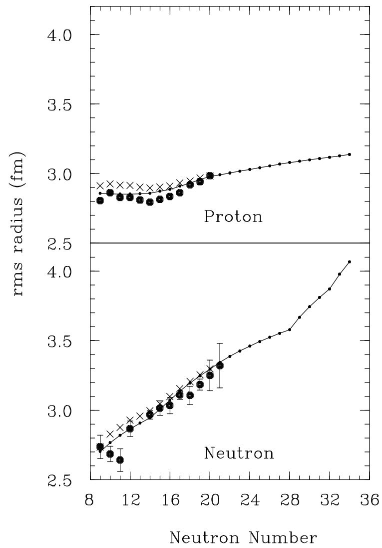

Figure 1: Calculated and measured proton and neutron rms radii as a function of neutron number of the Na isotopes. The calculations were based on the SGII Skyrme parametrization. The small dots and solid line correspond to the HF calculation with simple occupation numbers, and the crosses were obtained with the sd-shell occupation numbers. The solid points in the top panel are the experimental proton rms radii. The points with error bars in the bottom panel correspond to the experimental neutron rms radii extracted from the data.

a given nucleus may need to be modified. Thus, for ^{48}Ca we consider a modification which is derived from matching the SPE to the binding energy differences between the ^{48}Ca ground state and the single-particle states in the adjacent A=47 and A=49 isotopes. The three stages of calculation for the fp shell are indicated by D6 (the original shell-model interaction FPD6 [5]), D6* + HF, where * indicates that the monopole terms have been removed and HF indicates that the SPE have been replaced by HF single-particle energies, and D6* + HF*, where HF* indicates that the HF SPE have been modified as described. Applications are made to the nuclei $^{(47-60)}$Ca. A detailed comparison has been made for $^{(48)}$Ca including the electron scattering data for $^{(48)}$Ca. The level diagram is shown in Fig. 1. The experimental data is grouped into "Exp-fp", those positive parity levels which can be assigned to *(fp)* ^{8} configurations, "Exp-N", other levels which are probably negative parity, and "Exp-O", other levels which are probably positive parity or not known. KB indicates the interaction of Kuo and Brown [6]. Significantly better agreement with experiment is achieved than has been possible other available two-body interactions.

4 Coulomb displacement energies

One of the classic problems in nuclear structure physics is to understand the displacement energies of nuclei. The displacement energy is the binding energy difference between mirror nuclei (those with the same atomic number A but with the proton Z and neutron N numbers interchanged). If the nuclear force is charge symmetric, then this binding energy difference can be related to the well-understood Coulomb interaction between the protons. However, it was shown by Nolen and Schiffer [7] that there was a systematic

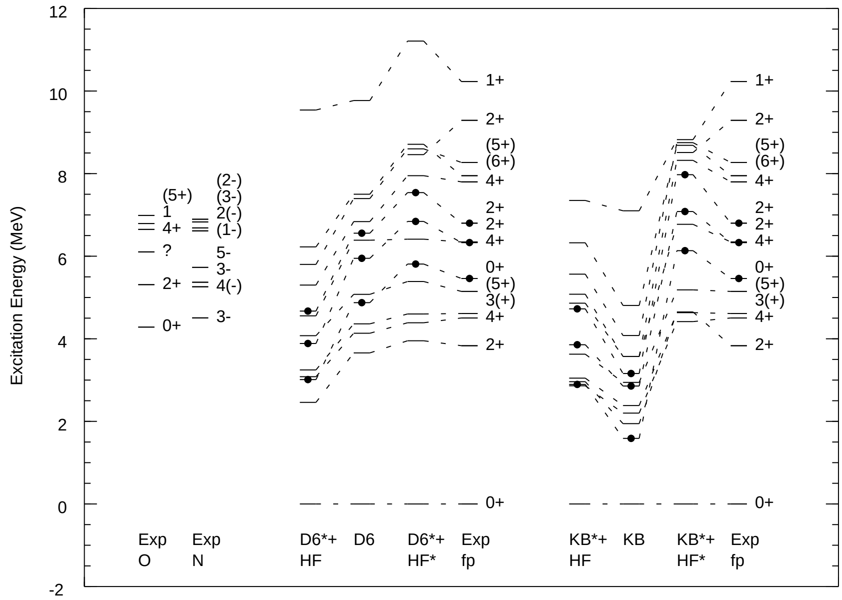

Figure 2: Energy levels for ^{48}Ca. See text for a discussion of the labels.

reduction in the experimental displacement energies compared to those calculated with a charge symmetric strong interaction (the Nolen-Schiffer anomaly). It is generally agreed that both nuclear correlations and a charge-symmetry breaking (CSB) strong interaction are important for its understanding.

We consider three modifications to the SKX Skyrme parameterization discussed in Ref. [1] : a) The addition of an exchange part of the Coulomb interaction, resulting in SKXce. The exchange part of the Coulomb interaction comes from the Slater approximation and is the first term of the density matrix expansion in the local density approximation.

$$V_{\text{Coul,exch}} = -x_c e^2 \left(\frac{3}{\pi}\right)^{1/3} \rho_{ch}^{1/3}, \tag{1}$$

where x_c is a parameter which can be used to modify its strength.

b) The strength of the exchange part is determined from displacement energy data. The modification of this strength is such that x_c is zero within its uncertainty, and for simplicity SKX is considered to have $x_c = 0$. We do not regard the $x_c = 0$ solution as evidence that the Coulomb exchange term itself is missing, but rather that there may be another term in the energy density functional, related to nuclear correlations, which happens to cancel the exchange term.

c) An s-wave charge-symmetry-breaking term (CSB) is added and fitted to the displacement energy data. The CSB modification of the Skyrme interaction is expressed as a change to the proton-proton (pp) and neutron-neutron (nn) s-wave interactions:

$$V^{pp}_{\text{Skyrme}} = t_0(1 - x_0)(1 + x_a)\delta$$

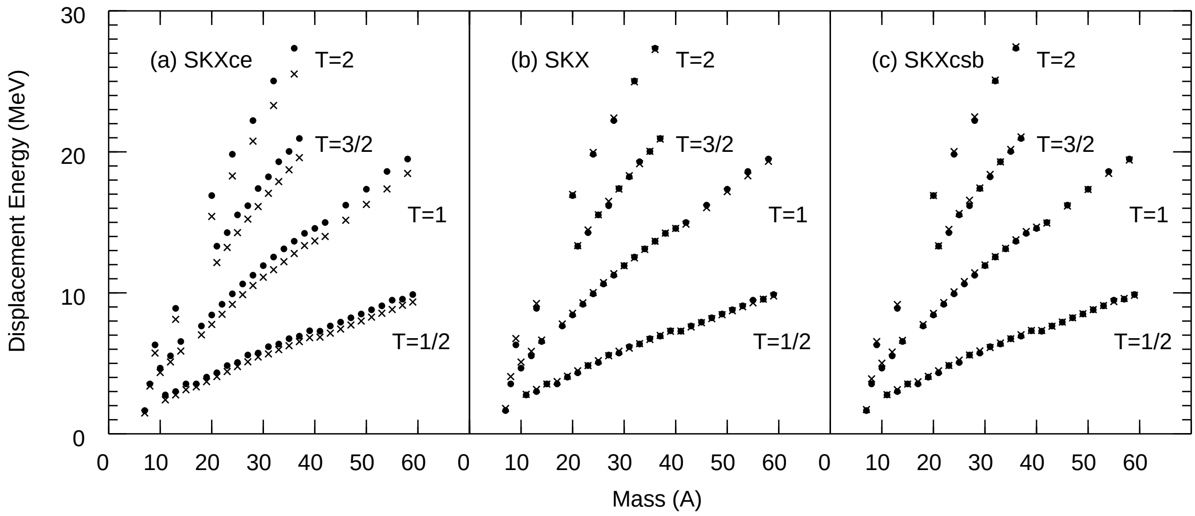

Figure 3: Displacement energies as a function of A for SKXce (with the normal Coulomb exchange term, i.e. $x_c = 1$), SKX (without the exchange term) and SKXcsb (with the exchange term and with a CSB interaction). The data are the filled circles and the calculations are the crosses.

and

$$V^{nn}_{\text{Skyrme}} = t_0(1 - x_0)(1 - x_a)\delta, \tag{2}$$

where x_a is a parameter to be determined from fits to the experimental data. The method has been applied to a data set comprising all bound known mirror pairs – (Z,N) and (N,Z) nuclei – in the mass region A = 7 to A = 59 [8]. The results for the measured displacement energies are shown in Fig. 3. Points are given for all cases with $A \geq 7$ where the experimental binding energies are known. The theoretical displacement energy is the difference between the total Hartree-Fock binding energies of the mirror nuclei. All calculations are constrained to be spherical, and the shell-model orbitals are filled in integer steps in the order in which they occur in the mass-dependent potential. For the SKXce comparison in Fig. 1(a), one observes the systematic deviation between experiment and theory associated with the Nolen-Schiffer anomaly. The experimental displacement energies are much better reproduced by the SKX (b) and SKXcsb (c) fits. The agreement between experiment and theory for SKX and SKXcsb are nearly identical. The differences between experiment and theory for SKX and SKXcsb have an rms value of about 100 keV for large A. The deviation with experiment becomes worse for light nuclei, and this is generally related to the breakdown of the mean-field approximation when the number of particles becomes small.

5 Masses of proton-rich nuclei relevant to the astrophysical rp process

Nuclear masses are among the most important input parameters in rp-process calculations, as they sensitively determine the balance between proton capture and the inverse process, (γ, p) photodisintegration. It is this (γ, p) photodisintegration that prevents the rp process from continuing via proton captures, once a nucleus close to the proton drip line is reached. This nucleus becomes then a "waiting point" as the rp process has to proceed at least in part, via the slow β^+ decay. The effective lifetime of the waiting points in the rp process determines the overall processing time scale, energy generation, and the final abundance distribution.

One-proton and two-proton separation energies, based on calculations of the nuclear masses, have been determined for proton-rich nuclei in the region A=41-75 [9]. The method is based on calculations of Coulomb displacement energies of mirror nuclei as in the previous section (assumed to be accurate within about 100 keV) in combination with the experimental masses of the neutron-rich nuclei, which are usually known to within 100 keV or better. The implications for the proton drip line and the astrophysical rp-process have been considered within the framework of a detailed analysis of the sensitivity of rp process calculations in type I X-ray burst models on nuclear masses.

The displacement energy is the difference in the binding energies of mirror nuclei for a given mass A and isospin T:

$$D(A,T) = BE(A,T_z^<) - BE(A,T_z^>), \tag{3}$$

where $T = \mid T_z^< \mid = \mid T_z^> \mid$, $BE(A,T_z^<)$ is the binding energy of the proton-rich nucleus and $BE(A,T_z^>)$ is the binding energy of the neutron-rich nucleus. The displacement energy can be much more accurately calculated than the individual BE in a variety of models since it depends mainly on the Coulomb interaction.

The single-particle states in proton-rich nuclei become unbound outside of the proton-drip line. In the nuclei we consider the single-particle states are unbound by up to about 2 MeV. Since 2 MeV is small compared to the height of the Coulomb barrier (about 6 MeV at a radius of 7 fm), the states are "quasi-bound" and have a small proton-decay width (on the order of keV or smaller). To obtain the quasi-bound wave functions we put the HF potential in a box with a radius of 20 fm and a depth of 20 MeV. The binding energies for the HF extrapolations for the proton-rich nuclei are given an error based upon the experimental error of the neutron-rich binding energy folded in quadrature with an assumed theoretical error of 100 keV. In the absence of experimental masses for the proton-rich nuclei, one often uses the masses based upon the Audi-Wapstra extrapolation (AWE) method [10]. The calculated displacement energies are shown in Fig. 4.

Our new calculations lead to tighter constraints on proton capture Q-values as compared with the Audi-Wapstra mass extrapolations. However, we are not able to improve upon the masses of nuclei with N=Z, and the relative large errors which remain for the masses of the ^{64}Ge and ^{68}Se waiting point nuclei provide the dominant uncertainty in the rp-process calculations. We find that the remaining mass uncertainties still lead to large uncertainties in calculations of X-ray burst light curves. Further experimental or theoretical improvements of nuclear mass data are necessary before observed X-ray burst light curves can be used to obtain quantitative constraints on ignition conditions and neutron

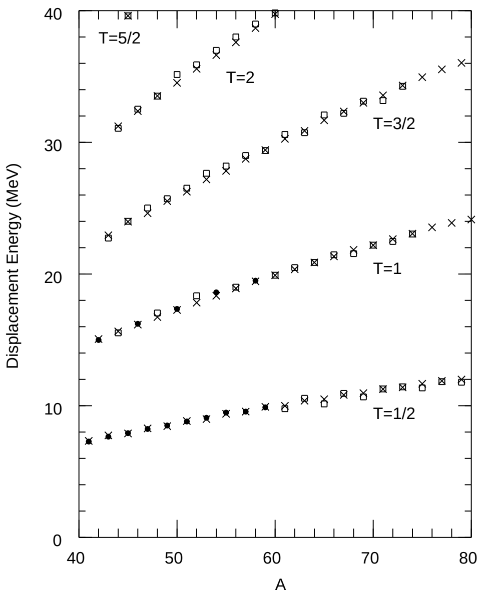

Figure 4: Calculated displacement energies (crosses) as a function of mass number. They are compared to experimental data (filled circles) and to values based upon the Audi-Wapstra extrapolations.

star properties. We also identify a list of nuclei for which improved mass data would be most important.

6 Interaction cross-sections for light neutron-rich nuclei

We have calculated interaction cross-sections and rms matter radii for nuclei with Z = 2-12 on a ^{12}C target in the Glauber model with matter densities obtained from the Skyrme Hartree-Fock model [11]. When one approaches the neutron drip line the matter radii are sensitive to the separation energies, especially for the low-l orbits. The separation energy also depends on the pairing and collective aspects of the residual interaction which are not taken into account in the HF mean field. Thus near the drip line we constrain the orbit occupations and separation energies in the Hartree-Fock calculations by the results of shell-model configuration mixing calculations and experimental data on binding energies and spectroscopic factors.
The interaction cross sections are compared with experiment in Fig. 5. The interaction cross-sections give excellent agreement with experiment, even for the halo nuclei, if all the calculated cross-sections are multiplied by 0.95. The empirical reduction factor of 0.95 may be attributed to an average of nuclear correlation effects for normal and halo nuclei.
In summary, it has been shown that the complete set of interaction cross-section data can be described by the Glauber model with matter densities obtained from mean-field models supplemented by constraints on the orbit occupation and separation energies of the most loosely bound valence orbits. Good agreement between experimental and calculated rms matter radii has also been obtained.

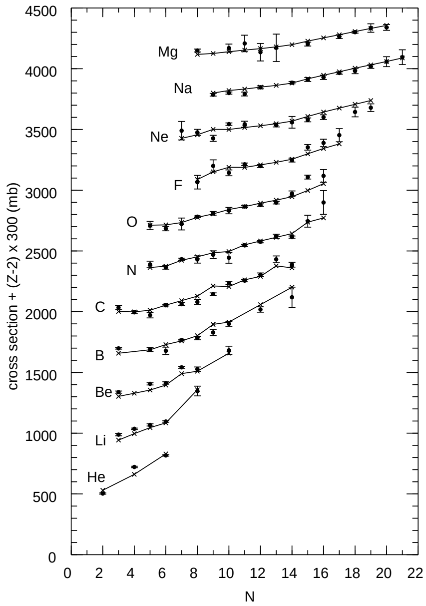

Figure 5: Calculated and experimental interaction cross sections. The values for Z are separated by the addition of 300(Z-2).

7 Nuclear charge densities and rms radii

Elastic electron scattering from nuclei has provided a great resource of experimental data with which to test models for nuclear ground states. It evolved from the early determinations of rms charge radii, to much more precise measurements in the 70's and 80's which have provided nearly model-independent determinations of the charge-density distributions of many nuclei.

Improving our capability of reproducing charge density distributions for stable nuclei accurately will enable extrapolations to exotic nuclei when such measurements become feasible. The charge density distributions in the mass range A = 12 to 209 and the associated nuclear radii have been calculated [12] for the purpose of comparison with available electron elastic scattering data. About 80 calculated charge-density distributions based on the new Skyrme SKX interaction, as well as an older parameterization, the SKM* (differing mainly in the density-dependent term), have been compared with experiment [13,14]. We succeeded in significantly improving the predictions of nuclear charge densities for a selected set of magic or semi-magic nuclei when the Hartree-Fock calculations are constrained to using shell-model occupation numbers. (See fig. 6) The level of agreement obtained with experiment in this way was within about 2% (for $r < 1$ fm)), which is also the level of accuracy of most measurements.

Subsequently charge density distributions were systematically calculated for various model spaces using shell-model occupations from large-basis shell-model calculations. In general very good agreement between theory and experiment is obtained. For lighter nuclei (mainly p-shell nuclei) there were larger deviations, and these can be probably be attributed to the fact that the mean-field approximation would be less valid for smaller numbers of nucleons. In general it was found that using occupation numbers from shell-model calculations gave significantly better improvement between theory and experiment.

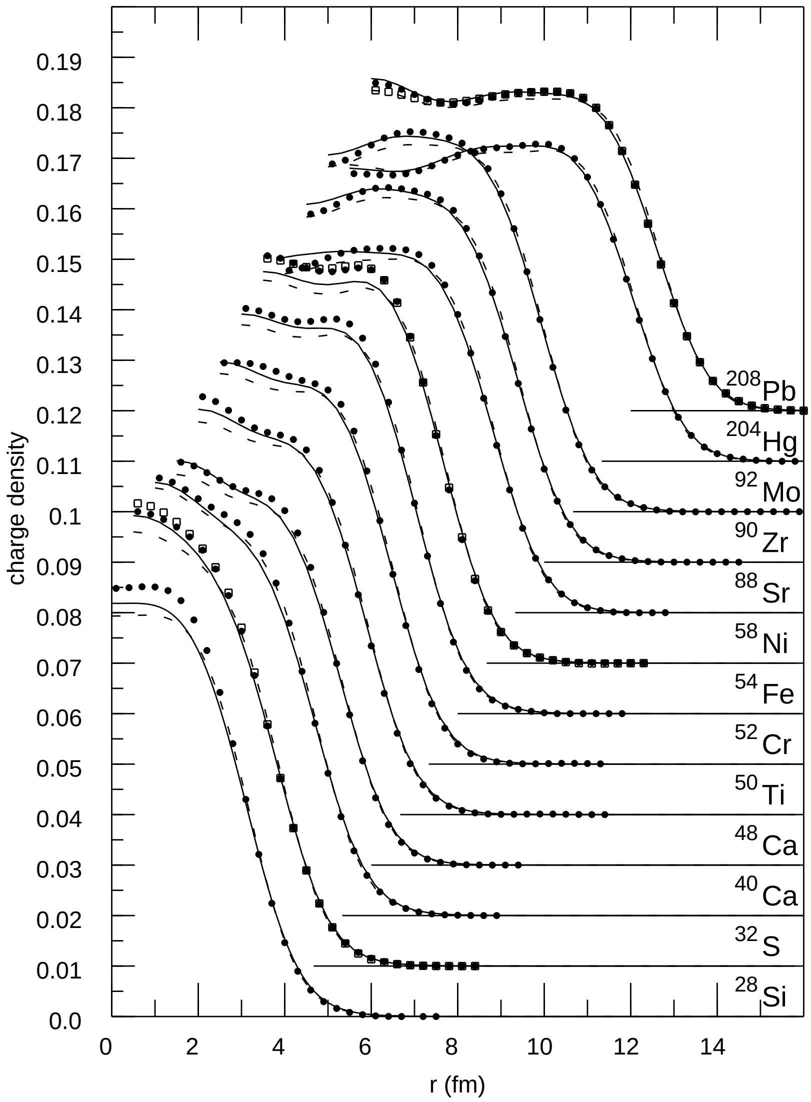

Figure 6: Experimental charge-density distributions (filled circles) compared with the SKX (dashed lines) and SKM* (solid lines) calculations. In both cases the occupation numbers for the non-closed-shell nuclei are obtained from valence configuration mixing calculations. The charge density units are in e fm^{-3}. Beyond ^{28}Si the curves and data have been progressively offset by 1 fm and 0.01 in the charge density.

8 Q-values for alpha decay of superheavy nuclei

New calculations of the alpha decay Q values for superheavy nuclei based on deformed Hartree-Fock calculations with the SKX Skyrme interaction have been made [15]. Agreement with experiment including the recently observed Z = 112, 114 and 116 decays is obtained at the rms level of a few hundred keV.

9 Conclusions

Good agreement has generally been found between experiment and theory in a variety of situations for the SKX type of interaction using the Hartree-Fock model. For light nuclei greater deviations have been observed, which probably relate to the inadequacy of the mean-field approximation for such cases. For displacement energies a charge-symmetry breaking term is required which can be readily be interpreted physically and which can explain the energy systematics of the data. The use of shell-model occupancies simulating configuration mixing gives consistently better agreement with experiment in all cases considered. The effects of nuclear correlations need to be taken into account in the long term, as evidenced by the improvements associated with using shell-model occupation numbers - possibly by an extension of the combined shell and Hartree-Fock models.

10 References

1. B. A. Brown. Phys. Rev. **C 58**, 220 (1998)
2. T. Suzuki et al. Phys. Rev. Lett. **75**, 3241 (1995)
3. B. A. Brown and W. A. Richter, Phys. Rev. **C 54**, 673 (1996)
4. B. A. Brown, W. A. Richter. Phys. Rev. **C 58**, 2099 (1998)
5. W. A. Richter, M. G. Van der Merwe, R. E. Julies and B. A. Brown, Nucl. Phys. Rev. **A 577**, 585 (1994)
6. T. T. S. Kuo and G. Brown, Nucl. Phys. **A 114**, 241 (1968)
7. J. A. Nolen, J. P. Schiffer, Ann. Rev. Nucl. Sci. **19** (1969) 471
8. B. A. Brown, W. A. Richter and R. Lindsay, Phys. Lett. **B 483**, 49 (2000)
9. B. A. Brown, W. A. Richter, H. Schatz, R. Clement, A. Volya, Phys. Rev. **C 65**, 045802(2002)
10. G. Audi and A. H. Wapstra, Nucl. Phys. **A 595**, 409 (1995)
11. B. A. Brown, S. Typel, W. A. Richter, Phys Rev. **C 65**, 014612 (2001)
12. W. A. Richter, B. A. Brown, Phys. Rev. **C 67**, 034317 (2003)
13. H. De Vries, C. W. De Jager, and C. De Vries, Atomic Data and Nuclear Data Tables **36**, 495 - 536 (1987).
14. G. Fricke, C. Bernhardt, K. Heilig, L. A. Schaller, L. Schellenberg, E. B. Shera and C. W. de Jager, Atomic Data and Nuclear Data Tables **60**, no. 2, 177 (1995).
15. S. Typel, B. A. Brown, private communication